

# ImmunoPET using engineered antibody fragments: fluorine-18 labeled diabodies for same-day imaging

Tove Olafsen · Shannon J. Sirk · Sebastian Olma · Clifton K.-F. Shen · Anna M. Wu

Received: 17 November 2011 / Accepted: 14 February 2012 / Published online: 6 March 2012  
© International Society of Oncology and BioMarkers (ISOBM) 2012

**Abstract** Combining the specificity of tumor-targeting antibodies with the sensitivity and quantification offered by positron emission tomography (PET) provides tremendous opportunities for molecular characterization of tumors *in vivo*. Until recently, significant challenges have been faced when attempting to combine antibodies which show long biological half-lives and positron-emitting radionuclides with comparably short physical half-lives, in particular  $^{18}\text{F}$  (half-life, 109 min). A fast and simple microwave-assisted method of generating *N*-succinimidyl-4- $^{18}\text{F}$ fluorobenzoate has been developed and employed for radiolabeling a small, rapidly targeting HER2-specific engineered antibody fragment, the cys-diabody. Using this tracer, HER2-positive tumor xenografts in mice were detected at 1–4 h post-injection by microPET. This confirms the rapid kinetics of  $^{18}\text{F}$ fluorobenzoyl cys-diabody localization, and demonstrates the feasibility of same-day immunoPET imaging. This approach can be broadly applied to antibodies targeting cell surface biomarkers for molecular imaging of tumors and should be highly translatable for clinical use.

**Keywords** Positron emission tomography · Radiochemistry · Antibody fragment · Small animal imaging · HER2 imaging

## Introduction

The lure of combining positron emission tomography (PET), which affords highly sensitive and potentially quantitative imaging of specific molecular targets in living organisms and patients, with the exquisite specificity and affinity offered by antibodies, is compelling. However, the reality of combining radioisotopes with relatively short physical half-lives and intact antibodies with correspondingly long biological half-lives has been more analogous to an irresistible force meeting an immovable object. The most commonly used positron-emitting radionuclide in current clinical use is fluorine-18. With a 109.8 min half-life,  $^{18}\text{F}$  is well suited for labeling small molecules such as  $^{18}\text{F}$ -2-fluoro-2-deoxy-D-glucose (FDG), which is widely used in clinical oncology and neurology for rapid imaging and assessment of metabolic activity.  $^{18}\text{F}$  has the added advantages of being a pure positron emitter, allowing more accurate quantitation of signal, and can be produced in biomedical cyclotrons, leading to widespread availability. Other positron emitting radioisotopes of naturally occurring elements including  $^{11}\text{C}$ ,  $^{13}\text{N}$ , and  $^{15}\text{O}$  have even shorter physical half-lives ( $T_{1/2}$ =20.4, 9.96, and 2.03 min, respectively). As a result, attempts to combine these short-lived radionuclides with antibodies whose biological half-lives extend from days to weeks are challenged by the need to achieve sufficient clearance and contrast between targeted tissues and background before the radioactive signal decays. Fortunately, these challenges are now being addressed on the radionuclide side through the use of longer-lived positron-emitting isotopes, as well as on the antibody side by producing engineered antibody fragments with accelerated biological kinetics [1, 2].

T. Olafsen · S. J. Sirk · S. Olma · C. K.-F. Shen · A. M. Wu (✉)  
Crump Institute for Molecular Imaging,  
Department of Molecular and Medical Pharmacology,  
David Geffen School of Medicine at UCLA,  
570 Westwood Plaza, CNSI 4335, Box 951770,  
Los Angeles, CA 90095-1770, USA  
e-mail: awu@mednet.ucla.edu

### Present Address:

S. J. Sirk  
Department of Chemistry, The Scripps Research Institute,  
10550 North Torrey Pines Road, BCC526,  
La Jolla, CA 92037, USA

### Present Address:

S. Olma  
URENCO Limited, Central Technology Group,  
Röntgenstrasse 4,  
48599 Gronau, Germany

Pioneering studies of immunoPET in the 1990s demonstrated the feasibility of PET imaging using antibodies radio-labeled with  $^{124}\text{I}$  (half-life, 4.2 days) [reviewed in 3, 4]. However, until recently, access to “exotic” positron emitters with longer physical half-lives, such as  $^{64}\text{Cu}$  (12.7 h),  $^{86}\text{Y}$  (14.7 h),  $^{76}\text{Br}$  (16.0 h), and  $^{89}\text{Zr}$  (3.2 d) and as well  $^{124}\text{I}$ , has been limited. Generator-produced  $^{68}\text{Ga}$  (68 min) has also been employed for PET imaging using antibody fragments [5, 6]. Availability of these and other diverse positron emitting radio-nuclides has improved significantly in the past few years. In parallel, widespread availability of clinical PET scanners (due to broad implementation of metabolic imaging utilizing [ $^{18}\text{F}$ ] FDG) has led to renewed interest in immunoPET imaging using intact antibodies.

Protein engineering strategies have been used to engineer antibodies specifically for imaging applications, with the goals of accelerating blood clearance, eliminating biological activity, improving diffusion and transport into target tissues, steering clearance to the hepatic or renal elimination pathways, and providing defined sites for conjugation of radioactive labels, while retaining high affinity toward their targets [1, 2]. In particular, engineered antibody fragments have provided solutions to the challenges of antibody imaging. For example, formats such as the minibody (a dimer of single-chain Fv [scFv] fragments fused to a human IgG  $\text{C}_{\text{H}3}$  domain) provide a bivalent, intermediate-sized (80 kDa) antibody fragment. Carcinoembryonic antigen (CEA)-specific minibodies reached peak uptake in LS174T CEA-positive tumors within 6 h and cleared with a terminal half life of 5.3 h in mouse models [7]. Even faster kinetics are provided by smaller fragments such as the diabody, a dimer of scFv fragments (55 kDa). An anti-CEA diabody achieved high uptake in LS174T tumors within 1–2 h of administration and cleared with 2.9 h terminal half-life [8]. Furthermore, calculation of an imaging figure of merit [9] predicted that if one wished to image using an antibody fragment labeled with  $^{18}\text{F}$ , the diabody would be the most suitable format, providing optimal imaging contrast at 1.4 h post-injection.

This prediction was confirmed by Cai et al. who coupled  $^{18}\text{F}$  to a diabody fragment and demonstrated rapid uptake and imaging of CEA-expressing tumor xenografts in mice by microPET [10]. Radiolabeling was accomplished by using *N*-succinimidyl-4- $^{18}\text{F}$ fluorobenzoate ( $^{18}\text{F}$ ]SFB) which reacts with the  $\epsilon$ -amino group of surface-exposed lysine residues on proteins, an approach described by Zalutsky et al. [11, 12].  $^{18}\text{F}$ fluorobenzoyl( $^{18}\text{F}$ ]FB)-labeled Mel-14F(ab')<sub>2</sub> fragments were produced and showed no loss of affinity, while the biodistribution results were highly similar to fragments radioiodinated using *N*-succinimidyl-4- $^{125}\text{I}$ iodobenzoate [11]. Applying the same strategy, a different tag, *N*-succinimidyl-4-[(4-nitrobenzenesulfonyl)oxymethyl]benzoate [13] was employed for  $^{18}\text{F}$ -labeling and biodistribution studies of an anti-Tac disulfide-stabilized Fv fragment [14].

Taking advantage of its bivalency and small size, Cai et al. applied the latter  $^{18}\text{F}$ -labeled diabody to evaluate its targeting and imaging by small animal PET. [ $^{18}\text{F}$ ]FB-anti-CEA diabody showed rapid tumor localization and provided high contrast images at 1, 2, and 4 h post-injection. In comparison, accumulation in control, antigen-negative C6 xenografts was very low [10]. These studies clearly demonstrated the feasibility of same-day immunoPET using  $^{18}\text{F}$ -labeled diabodies.

In order to implement a routine, practical labeling procedure for engineered antibody fragments for imaging, additional refinements are necessary. Typically, bench-scale production of [ $^{18}\text{F}$ ]SFB requires a lengthy, 2-h synthesis involving three steps, followed by a 35-min diabody labeling and purification. Initial yields and specific activities were low, requiring starting activities of 0.5–1 Ci in order to obtain sufficient  $^{18}\text{F}$ -labeled diabodies for imaging studies in mice. One strategy to increase the efficiency and speed of producing [ $^{18}\text{F}$ ]SFB has been to adapt the synthesis to a three-step, one-pot, microwave-assisted method (Fig. 1a), which is followed by either a single cartridge or high-performance liquid chromatography (HPLC) purification [15]. Total synthesis and purification time was reduced to 40 min, with a decay-corrected radiochemical yield of 17–31% over 30 syntheses. This robust and reliable method to produce [ $^{18}\text{F}$ ]SFB for radiolabeling biomolecules, including diabodies, provides a simple and general path to immunoPET tracers based on antibodies of any desired specificity.

The present work is based on a HER2-specific diabody previously modified to include C-terminal cysteine residues; the HER2 cys-diabody (Cys-Db) exists as a stable, covalent dimer (Fig. 1b) [16]. We describe  $^{18}\text{F}$  radiolabeling by reaction of [ $^{18}\text{F}$ ]SFB with the  $\epsilon$ -amino groups of lysine residues on the anti-HER2 Cys-Db. Performance of [ $^{18}\text{F}$ ]FB-Cys-Db was evaluated by conducting biodistribution and microPET studies on mice bearing HER2-expressing human breast cancer xenografts.

## Materials and methods

### Cell lines

The transfected human breast tumor cell line, MCF-7/HER2 [17] was propagated in Dulbecco's modification of Eagle's medium (DMEM) supplemented with 4.5 g/L glucose, 1 mM L-glutamine, 1 mM sodium pyruvate, 0.1 mM non-essential amino acids (Cellgro®; MediaTech Inc., Manassas, VA, USA) and 10% fetal bovine serum (FBS). The rat glioma cell line C6 (CCL-107; American Type Culture Collection, Manassas, VA, USA) was propagated in deficient DME high glucose medium without phenol red (Irvine Scientific, Santa Ana, CA, USA) supplemented with 5% FBS. Both media were also supplemented with 1% of

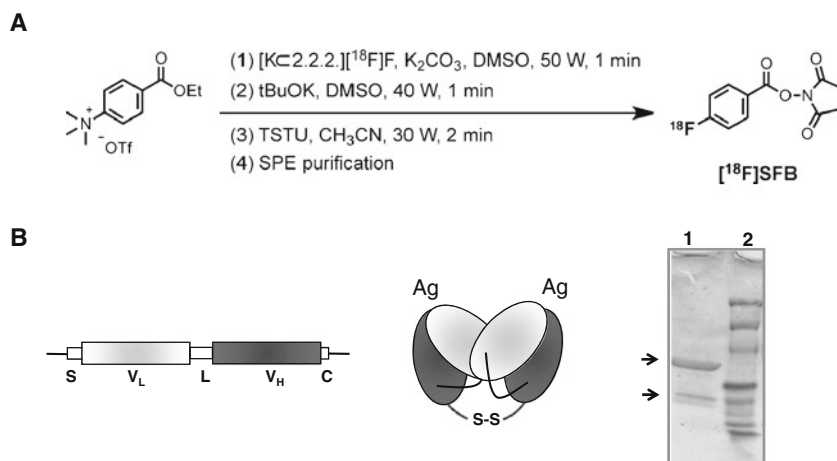


**Fig. 1**  $[^{18}F]$ SFB synthesis and the anti-HER2 Cys-Db. **a** The reaction steps in the one-pot microwave assisted  $[^{18}F]$ SFB synthesis. **b** Schematic presentation of the Cys-Db gene construct and protein. *S* signal sequence, *V<sub>L</sub>* variable light, *L* GGGGS linker, *V<sub>H</sub>* variable heavy, *C* GGC extension. The assembled, cross-paired protein structure and sites where antigen binds (Ag) are shown in the *center panel*. The Cys-Db is covalently bound by a disulfide bridge linking the C-termini. Migration

of the  $[^{18}F]$ FB-Cys-Db under nonreducing conditions in SDS-PAGE is shown (*right panel* Coomassie-stained). The major band in *1* represents the  $[^{18}F]$ FB-Cys-Db which was associated with 82.5% of the total radioactivity. The lower molecular weight band most likely represents noncovalently bound diabody and comprised 14.2% of the total radioactivity. A faint band of higher molecular weight represented 3.3% of the activity. *2* molecular weight standards

Gibco™ penicillin–streptomycin–glutamine (100× liquid; Invitrogen Corp., Carlsbad, CA, USA).

#### Microwave reactor setup for $[^{18}F]$ SFB synthesis

The microwave-assisted reactions were performed in a single-mode microwave reactor (Discover, CEM, Matthews, NC, USA) capable of continuous microwave irradiation. This instrument includes temperature sensing and control, adjustable power output (0–300 W), and applicable gas cooling. The microwave cavity from the microwave system (Discover, CEM, Matthew, NC, USA) was modified such that a 5-mL V-vial (Reactivial, Wheaton Scientific, Millville, IL, USA), equipped with a magnetic stir bar and a polyaryletheretherketone (PEEK) adaptor (Eckert & Ziegler, Berlin, Germany) for tubing connection, could be placed inside. The metallic lid of the microwave cavity was also modified to accommodate the 5-mL V-vial. A custom-made radiochemistry system gives remote access to the vessel. It comprises seven electrically actuated solenoid valves, each connected to the V-vial by a PEEK adapter through 1/16" Teflon tubing. Three ports were used for reagent delivery with tubing equipped with a Luer adapter (Cole–Parmer, Vernon Hills, IL, USA). One port served as a solution output, where the tubing was extended to the bottom of the vial. Another one permitted venting of the vial. The final two ports were connected to pressurized nitrogen or a vacuum pump, respectively. This system was designed to facilitate a semi-automated radiosynthesis operation in a closed hot cell, which could be remotely controlled by an operator using Synergy software (CEM) and a LabView

(National Instrument, Austin, TX, USA) program, both on a touch screen computer.

#### Microwave-assisted $[^{18}F]$ SFB synthesis

Briefly, dried potassium Kryptofix 2.2.2  $[^{18}F]$ fluoride ( $[K \subset 2.2.2][^{18}F]F$ ) salt was prepared by adding an aliquot of aqueous  $[^{18}F]$ fluoride solution (100  $\mu$ L) to Kryptofix 2.2.2 (10 mg) and an aqueous solution of potassium carbonate (1 M, 13  $\mu$ L). The mixture was then diluted with anhydrous acetonitrile (0.9 mL, biotechnology grade) and transferred to the reactor. The solvent was evaporated by a stream of nitrogen under microwave irradiation (20 W, 3 min) and the drying sequence was repeated again with anhydrous acetonitrile (1 mL). In order to make the first intermediate ethyl-4- $[^{18}F]$ fluorobenzoic acid ( $[^{18}F]$ FBA), a solution of ethyl 4-(N,N,N-trimethylammonium)benzoate triflate (2.5 mg) in DMSO (300  $\mu$ L) was added to the V-vial containing the dried  $[K \subset 2.2.2][^{18}F]F$  salt and the reaction was conducted for 1 min with a microwave energy of 50 W. This was followed by addition of potassium tert-butoxide (10 mg) in DMSO (300  $\mu$ L) and another minute at 40 W that cleaved off the ethyl ester group to yield  $[^{18}F]$ FBA. To convert  $[^{18}F]$ FBA into the form of *N*-hydroxysuccinimide ester, O-(*N*-succinimidy)-N,N,N',N'-tetramethyluronium tetrafluoroborate (30 mg) in anhydrous acetonitrile (2.5 mL) was added to  $[^{18}F]$ FBA and stirred for 2 min under microwave heating (30 W). The resulting crude product solution was acidified with an aqueous solution of acetic acid (5%, 8 mL) and trapped on a Merck EN cartridge (200 mg, conditioned

with 10 mL of ethanol and 10 mL of 5% acetic acid before use). After the cartridge was washed with a mixture of acetonitrile–water (1:2 ratio), [ $^{18}\text{F}$ ]SFB was eluted with diethyl ether (3 mL). The solvent was evaporated and [ $^{18}\text{F}$ ]SFB was redissolved in phosphate buffered saline (PBS, pH 7.4) for use in coupling of diabodies. The total synthesis time was about 40 min. The decay-corrected radiochemical yields (d. c. RCY) of [ $^{18}\text{F}$ ]SFB ranged from 17% to 31% with a radiochemical purity of >95% based on HPLC analysis (specific activity: *ca* 0.2–1 Ci/ $\mu\text{mol}$ ). An improved method of microwave-assisted one-pot synthesis of *N*-succinimidyl-4[ $^{18}\text{F}$ ]fluorobenzoate was later established and resulted in increased RCYs of  $35 \pm 5\%$  [15].

#### [ $^{18}\text{F}$ ]SFB conjugation to anti-HER2 Cys-Db and purification

The generation, purification, and characterization of the anti-HER2 Cys-Db have been described elsewhere [18]. For [ $^{18}\text{F}$ ]SFB labeling of anti-HER2 Cys-Db, 200  $\mu\text{g}$  of protein in 500  $\mu\text{L}$  of 50 mM sodium borate buffer (pH 8.5) was added to 100  $\mu\text{L}$  of [ $^{18}\text{F}$ ]SFB in PBS (pH 7.4) and incubated at room temperature for 30–45 min. For HPLC separation, 400  $\mu\text{L}$  of the reaction mixture was subjected to preparative size exclusion chromatography using a Biosep SEC S-2000 column (Phenomenex, Torrance, CA, USA). Separation was conducted in PBS and eluted fractions of 400  $\mu\text{L}$  each were collected and analyzed. Microspin column purification was performed by loading 75  $\mu\text{L}$  aliquots of reaction mixture onto Micro Biospin 6 columns (BioRad Laboratories, Hercules, CA, USA) and centrifugation. The total synthesis time (including [ $^{18}\text{F}$ ]SFB synthesis) was *ca* 100 min and overall d. c. RCY of [ $^{18}\text{F}$ ]FB-Cys-Db was *ca* 1.8–2.5%.

#### Radiochemical purity and immunoreactivity

The radiochemical purity was determined by instant thin layer chromatography (ITLC) using Monoclonal Antibody ITLC Strips (Biodex Medical Systems, Shirley, NY, USA). In order to determine the amount of the radiolabeled fraction actually associated with the Cys-Db, nonreduced radiolabeled protein was electrophoresed on a 4–20% pre-cast sodium dodecyl sulfate polyacrylamide gel electrophoresis (SDS-PAGE) gel (BioRad Laboratories) and stained with Instant Blue (Expedeon, San Diego, CA, USA). Visible bands were individually excised and counted in a Wallac WIZARD Automatic Gamma Counter (PerkinElmer Life and Analytical Sciences Inc., Boston, MA, USA). Immunoreactivities were determined by cell binding in duplicate to MCF-7/HER2 and C6 (HER2 negative) cells suspended in PBS/1% FBS to a final concentration of  $1\text{--}3 \times 10^6$  cells/mL per 500  $\mu\text{L}$ /sample. Between 50,000 and 100,000 cpm of [ $^{18}\text{F}$ ]FB-Cys-Db was added to the cell suspensions, and

incubated for 1 h at room temperature in a Labquake rotator. Cells were pelleted at  $3,000 \times g$  in a microcentrifuge for 15–30 min, washed with PBS/1% FBS, and pelleted again. The activities in the supernatants/washes and in the cell pellets were measured in the gamma counter.

#### Tumor xenografts

All animal handling was performed under protocols approved by the University of California, Los Angeles Chancellor's Animal Research Committee. One day prior to tumor implantation, athymic nude (nu/nu) female mice (approximately 12 weeks old; Charles River Laboratories International Inc., Wilmington, MA, USA) were injected in the right hind flank muscle with 50  $\mu\text{L}$  estradiol valerate (20 mg/mL; Bristol-Myers Squibb, New York, NY, USA). Tumors were established in the shoulder region by subcutaneous injection of  $2 \times 10^6$  MCF-7/HER2 cells suspended in 50  $\mu\text{L}$  unsupplemented DMEM and 50  $\mu\text{L}$  matrigel (BD Biosciences, San Jose, CA, USA). A total of five mice were implanted with MCF-7/HER2 cells. Two of these mice were also implanted with  $2 \times 10^6$  C6 cells (resuspended in 100  $\mu\text{L}$  unsupplemented medium) on the opposite shoulder. Tumors were allowed to grow for 2–3 weeks prior to imaging and biodistribution studies.

#### MicroPET/CT imaging and image analysis

Mice were injected via the tail vein with [ $^{18}\text{F}$ ]FB-Cys-Db and imaged in one bed position in a Focus 220 microPET scanner (Siemens Preclinical Solutions, Knoxville, TN, USA) followed by a 10 min scan in the microCATII (Concorde Microsystems, Knoxville, TN, USA) for anatomical reference. During imaging, mice were in a prone position on the bed, immobilized by anesthetization using 1.5–2% isoflurane. A 2-h dynamic scan was carried out with one mouse, followed by 10-min static scans at four mice and 6 h post-injection (p.i.). Static scans of 20 and 30 min were performed with another three mice at 4 and 6 h, and with one mouse at 4 h p.i.

MicroPET images were reconstructed using a filtered backprojection algorithm [19] and coregistered with microCT scans to yield a single image that was displayed using AMIDE [20]. One volume of interest (VOI; sphere;  $x, y, z = 3 \times 3 \times 3$  mm) was drawn over the tumor, heart, liver, kidney, muscle (soft tissue), and bladder. Two-hour time activity curves in the various tissues were obtained from the dynamic images. In order to determine the blood clearance rate, one VOI (ellipsoidal;  $x, y, z = 1.4 \times 1.2 \times 2.4$  mm) was drawn over the left ventricle of the heart. The VOI statistics were analyzed using the Kinetic Imaging System [21] to calculate the alpha and beta half-lives. The positive tumor-to-tissue ratios were determined for individual mice

at 2 h ( $n=1$ ), 4 h ( $n=5$ ), and 6 h ( $n=4$ ) p.i. The mean ratios and standard deviations at 4 and 6 h were calculated.

### Biodistribution

Following the final scan, mice were euthanized, and major organs dissected and weighed. The radioactivity in blood and in excised tumors and organs was counted in the gamma counter. The percent-injected dose per gram (% ID/g) in each tissue was determined after correcting for decay to the time of injection. The mean values and standard deviations in MCF-7/HER2 tumor, blood, liver, spleen, kidneys, lungs, and carcass at 6 h p.i. were calculated from four mice. Results were used to calculate tumor-to-organ and tumor-to-blood ratios. Significance testing was done at 0.05 confidence level using two-tailed Student's *t* test.

## Results

### Microwave-assisted [ $^{18}\text{F}$ ]SFB synthesis

We have developed a facile, one-pot synthesis of [ $^{18}\text{F}$ ]SFB based on a three-step, microwave-assisted non-aqueous radiochemical process using a new anhydrous deprotection method. Microwave heating enables a rapid transformation in each step—[ $^{18}\text{F}$ ]fluorination, deprotection, and activation (Fig. 1a) were each complete within 1–2 min, thereby greatly shortening the total reaction time. As a result, including purification on a Merck EN cartridge, the total synthesis time for the microwave-assisted one-pot process is 35–40 min. In these studies, the radiochemical yields of [ $^{18}\text{F}$ ]SFB ranged from 13% to 24% with a radiochemical purity of >95% following cartridge purification and radio-HPLC. Following elution with diethyl ether, evaporation of solvent, and redissolving in PBS (pH 7.4), the final [ $^{18}\text{F}$ ]SFB was stable for at least 2 h according to radio-HPLC as shown in [22].

### Radiochemical purity and immunoreactivities of anti-HER2 [ $^{18}\text{F}$ ]FB-Cys-Db

Initial conjugation of [ $^{18}\text{F}$ ]SFB resulted in radiochemical purity of 4.8% before purification, which improved to 98.8% after HPLC purification. The immunoreactivity was 32.2% and specificity was demonstrated by competitive cell binding, which resulted in a 75% decrease in binding. In subsequent conjugation reactions, radiochemical purities were 6.6–9.4% prior to purification. Spin column versus HPLC purifications yielded mean radiochemical purities of 67.9( $\pm$ 13.0)% ( $n=11$ ) and 94.7( $\pm$ 4.8)% ( $n=8$ ) and mean immunoreactivities of 59.0( $\pm$ 10.0)% ( $n=4$ )

and 52.3( $\pm$ 21.9)% ( $n=5$ ), respectively. Less than 1% activity was associated with the C6 control cells.

The radiolabeled fraction associated with the [ $^{18}\text{F}$ ]FB-Cys-Db was determined by measurement of the activity in the bands present on an SDS-PAGE of an HPLC-purified radiolabeled protein with a radiochemical purity of 83.7% (Fig. 1b, right). Counting revealed that 82.5% of the activity was associated with the band that represented the Cys-Db, and that the remaining radioactivity was associated with higher (3.3%) and lower (14.2%) molecular weight bands.

### MicroPET imaging of anti-HER2 [ $^{18}\text{F}$ ]FB-Cys-Db

MicroPET images with the anti-HER2 [ $^{18}\text{F}$ ]FB-Cys-Db were obtained from five mice carrying MCF-7/HER2 breast cancer xenografts. Two of these mice also carried HER2-negative C6 control tumors. The mean mass of the positive tumors was 150.8 ( $\pm$ 111.1)mg and ranged from 62 to 268 mg. The two negative tumors were 58 and 34 mg in mass. All mice were injected with spin column purified [ $^{18}\text{F}$ ]FB-Cys-Db. The amount of radioactivity administered ranged from 31 to 82  $\mu\text{Ci}$ .

One mouse was subjected to a 2-h dynamic scan followed by static scans at 4 and 6 h p.i. As can be seen in Fig. 2a, the positive tumor was clearly delineated at 2 h and the signal in the tumor increased at 4 h p.i. At 6 h, the tumor signal was still strong with the overall background activity reduced. However, the signals in the kidneys and bladder were still high. Time activity curves revealed retention and a slight increase of activity in the tumor during the first 2 h p.i. whereas steady decreases were seen in the kidney and soft tissue (Fig. 2b). Rapid loss of activity was observed in all the tissues over time; but at 6 h, the strongest signal remained in the positive tumor. A VOI drawn over the left ventricle revealed that the [ $^{18}\text{F}$ ]FB-Cys-Db cleared rapidly from the blood during the first 2 h (Fig. 3). The  $T_{1/2\alpha}$  and  $T_{1/2\beta}$  calculated from the images of this animal were 0.91 and 58.95 min, respectively.

Images from an additional three mice scanned at 4 and 6 h p.i. are shown in Fig. 4. The positive tumor (right shoulder) was clearly delineated in all three animals at 4 h, with some activity visible in the negative tumors (left shoulder) in mouse 1 and 2. However, at 6 h, no activity was seen in the negative tumors, while the positive tumor still exhibited a strong signal. Nonspecific background activity, predominantly in the kidneys and the bladder, was seen in all animals at both 4 and 6 h p.i. VOI analysis of the mice bearing both HER2-positive and HER2-negative tumors revealed an approximate twofold increase in positive-to-negative tumor signal with a ratio of about 1.5:1 at 4 h p.i. and about 3:1 at 6 h p.i. Table 1 shows the positive tumor-to-tissue (blood, liver, kidney, muscle, and bladder) VOI ratios at 4 and 6 h p.i. As expected for a rapidly clearing antibody

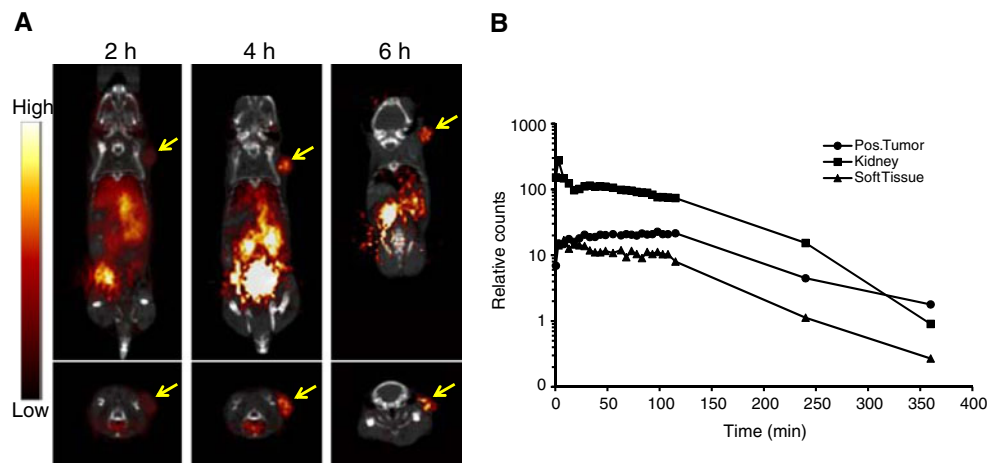


**Fig. 2** MicroPET images and time activity curves. **a** Coronal and transverse images of a mouse with an MCF-7/HER2 tumor on the right shoulder (*arrow*) serially imaged at 0–2, 4, and 6 h p.i. The mouse was injected with 82  $\mu$ Ci of [ $^{18}$ F] FB-anti-HER2 Cys-Db that showed

63% immunoreactivity. Each image is individually scaled. Images are not corrected for radionuclide decay. **b** Time–activity curves of the positive MCF-7/HER2 tumor, kidney and soft tissue, derived from drawn VOIs on the dynamic 0–2 h, and static 4 and 6 h scans

fragment, the ratios are highest at 6 h in all tissues, except bladder.

#### Tissue biodistribution

Biodistribution data were obtained from four mice at 6 h p.i. and are presented in Fig. 5 as % ID/g, with the positive tumor-to-tissue ratios indicated below. The mean tumor uptakes were  $2.87(\pm 0.43)\%$  ID/g for positive tumors and 0.7 and 1.25% ID/g (mean 1% ID/g) for the negative tumors, resulting in a mean positive-to-negative tumor ratio of 2.9:1. The kidneys had the next highest uptake with  $2.33:1(\pm 0.91)\%$  ID/g (tumor/normal ratio of 1.2:1). The blood and lung had 1–2% ID/g (T/N ratios of 1.7:1 and 2.5:1, respectively) whereas liver, spleen and carcass were all below 1% ID/g (T/N ratios were >5). The positive tumor uptake was significantly higher ( $p < 0.05$ ) than the uptakes in all the organs, with the exception of the kidney ( $p = 0.3214$ ).

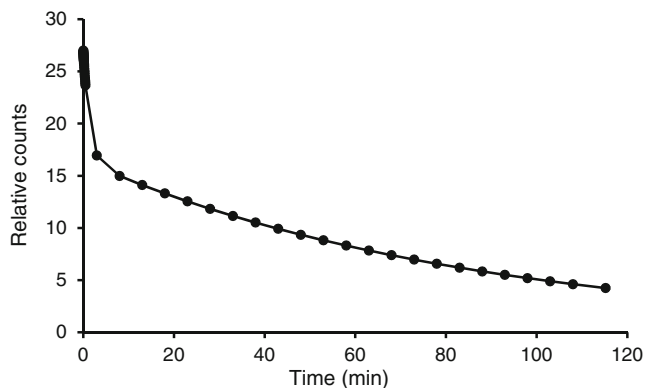


**Fig. 3** Blood clearance curve of [ $^{18}$ F] FB-anti-HER2 Cys-Db from 0 to 2 h p.i. derived from a VOI drawn over the left ventricle

#### Discussion

Microwave-assisted synthesis of [ $^{18}$ F]SFB provides a robust approach for radiolabeling engineered antibody fragments such as the HER2-specific cys-diabody, paving the way for

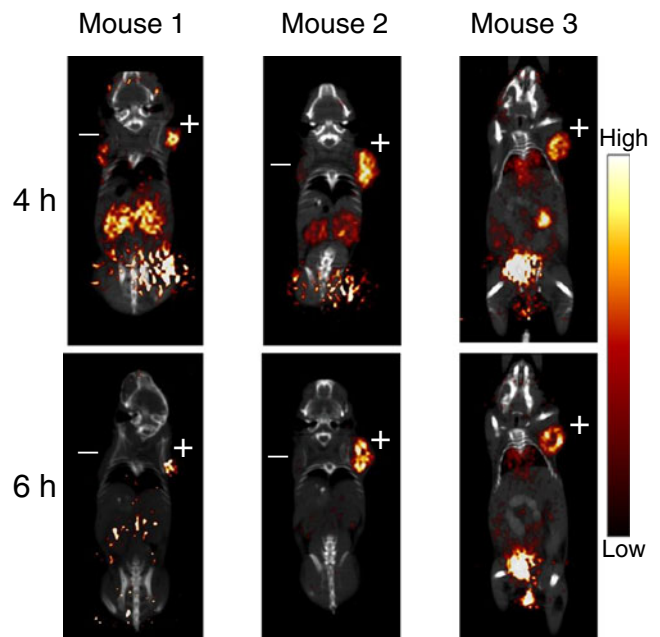


**Fig. 4** Coronal microPET images of three mice serially imaged at 4 and 6 h p.i. of [ $^{18}$ F] FB-anti-HER2 Cys-Db. Mouse 1, with C6 (58 mg, *left*) and MCF-7/HER2 (62 mg, *right*) xenografts, was injected with 34.4  $\mu$ Ci. Mouse 2, also with C6 (34 mg, *left*) and MCF-7/HER2 (268 mg, *right*) xenografts, was injected with 30.5  $\mu$ Ci. Images were acquired for 20 min at 4 and 6 h p.i. Mouse 3 with MCF-7/HER2 (276 mg, *right*) tumor only was injected with 67.1  $\mu$ Ci and imaged for 30 min at 4 and 6 h. Each image is individually scaled. Images are not corrected for radionuclide decay

**Table 1** Mean tumor (T) to tissue ROI ratios (SD) at 4 and 6 h

	4 h (n=5)	6 h (n=4)
T:Blood	1.25 (0.34)	1.83 (0.82)
T:Liver	2.09 (0.57)	3.13 (1.03)
T:Kidney	0.83 (0.49)	1.19 (0.73)
T:Muscle	5.50 (1.53)	6.87 (1.08)
T:Bladder	0.02 (0.01)	0.07 (0.06)

same-day imaging by immunoPET. There are three major advantages of this approach: (1) the microwave approach provides highly efficient energy transfer resulting in significantly shorter heating times; (2) the non-aqueous deprotection step makes one-pot synthesis feasible, and (3) integration with a remote-control system including cartridge separation makes routine production of high activities possible. As a result, the entire radiosynthesis required only 30–45 min and reproducibly furnished radiochemical yields of 13–24%, with radiochemical purity >95% following solid phase extraction. An advantage of this method over the conventional procedure is that [ $^{18}\text{F}$ ]SFB synthesis can be performed in a simple manual setup or in an automated radiochemistry module possessing a basic single-reactor configuration, such as the systems used for producing [ $^{18}\text{F}$ ]FDG.

Routine availability of [ $^{18}\text{F}$ ]SFB made it possible to conduct repeated radiolabeling and imaging studies with the anti-HER2 Cys-Db. Over a series of ten radiolabelings, coupling efficiencies ranged from 6.6% to 9.4%. We compared size exclusion HPLC to a spin column approach for purification of the radiolabeled protein; the HPLC method yielded [ $^{18}\text{F}$ ]FB-Cys-Db of high radiochemical purity. However, in the end this approach was not practical since it led to significant dilution, requiring concentration of the product prior to injection into the mice. Cell-based immunoreactivity, using either purification method, of the radiolabeled anti-HER2 Cys-Db

was comparable to previously reported cell-based immunoreactivities of other radiolabeled diabodies [10, 23, 24].

Dynamic and static microPET scans in five tumor-bearing mice demonstrated that [ $^{18}\text{F}$ ]FB-anti-HER2 Cys-Db rapidly targeted HER2+ tumors, which were visible at 2, 4, and 6 h following intravenous administration. Volume-of-interest analysis, as well as biodistribution data collected at the end of the series of scans, showed preferential uptake of probe in tumors overexpressing HER2 compared to control tumor ( $n=2$ ), and excellent tumor-to-normal tissue ratios for all organs ( $n=4$ ). Thus, the combination of  $^{18}\text{F}$  with an anti-HER2 Cys-Db which exhibits rapid tumor targeting and accelerated blood clearance results in an antibody-based PET tracer suitable for same-day imaging.

A different anti-HER2 diabody, C6.5, was previously evaluated by immunoPET following radioiodination with  $^{124}\text{I}$ , labeled either using Iodogen or SHPP [25]. In biodistribution studies of SCID mice bearing SKOV-3 xenografts, peak uptake of 9.8% ID/g was obtained in the tumor at 4 h, dropping to 6.3% and 3% ID/g at 24 and 48 h, respectively. The tumor-to-blood ratio increased from 6.7 at 24 h to 13.4 at 48 h. However, increased  $^{124}\text{I}$  activity was noted in the stomach and thyroid at later time due to metabolism and reuptake of freed radioiodine. For this reason, a residualizing labeling strategy (using SHPP) was also evaluated. In SCID mice bearing MDA-361/DYT2 xenografts, uptake was 0.9% ID/g with the indirectly (SHPP) labeled diabody, and 1.5% ID/g with directly (Iodogen) labeled diabody at 48 h p.i. with tumor-to-blood ratios of 3.1 and 6, respectively. The lower tumor retention with the SHPP labeled diabody was explained by decreased immunoreactivity. Overall lower tumor retention in MDA-361/DYT2 vs. SKOV-3 xenografts was attributed to the HER2 expression levels on the cells ( $\sim 1 \times 10^6$  vs.  $3.75 \times 10^5$  HER2/cell). In the current work, the [ $^{18}\text{F}$ ]FB-anti-HER2 diabody, derived from trastuzumab, reached  $\sim 3\%$  ID/g at 6 h in MCF-7/HER2 xenografts

**Fig. 5** Ex vivo mean biodistribution at 6 h ( $n=4$ ). Error bars standard deviations, asterisk significance ( $p < 0.05$ , two-tailed  $t$  test). The positive tumor-to-tissue ratios are shown

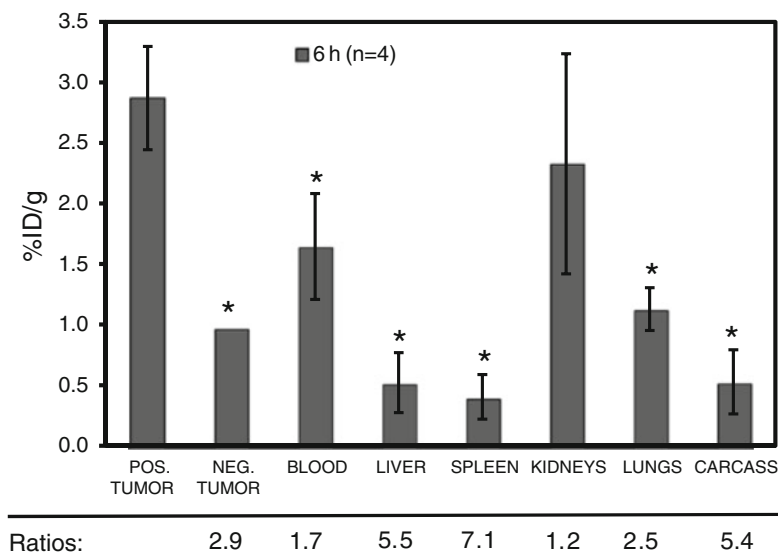


(Fig. 5). This difference in tumor retention cannot be attributed to HER2 expression, as the number of copies on MCF7/HER2 is similar to that of SKOV-3 [26]. The difference may be due to the difference in affinity and off-rates between the two antibody fragments, as 3% ID/g of the C6.6 diabody was retained in the tumor at 48 h p.i. Indeed, a reformatted C6.5 IgG has an affinity of  $5.4 \times 10^{-11}$  M [27], whereas trastuzumab has a reported affinity of  $5 \times 10^{-9}$  M. Alternatively, the [ $^{18}\text{F}$ ]FB-anti-HER2 cys-diabody might be undergoing metabolism and release of the radiolabel. Despite the relatively low uptake [ $^{18}\text{F}$ ]FB-anti-HER2 diabody, the positive-to-negative tumor ratio was 2.9:1 and the positive tumor-to-blood ratio was 1.7:1 at 6 h p.i., which allows delineation of HER2 positive tumors at an early time point. An alternative approach is to employ even smaller HER2-specific proteins such as Affibodies. A series of very high affinity, monovalent HER2-specific Affibodies have been labeled with a broad spectrum of radionuclides for PET and SPECT imaging [28]. In particular, Baum et al. [29] evaluated  $^{68}\text{Ga}$ -labeled ABY-002 in patients with excellent identification of tumors by PET within 2–3 h p.i. However, retention of activity in both kidneys and liver was observed. HER2-specific Affibodies have been radiolabeled site-specifically using *N*-[2-(4-[ $^{18}\text{F}$ ]fluorobenzamido)ethyl] maleimide [30, 31] or using aldehyde-aminooxy chemistry [32]. These studies reinforce the growing need for rapid and simple methods for  $^{18}\text{F}$ -radiolabeling of small targeting proteins.

The current work extends results observed with two other [ $^{18}\text{F}$ ]FB-labeled diabodies, with specificity for CEA or prostate stem cell antigen [10, 22]. In all three cases, antigen-positive tumor xenografts were readily visualized 1–4 h after administration of [ $^{18}\text{F}$ ]FB-diabodies. Combined, these studies open a path to practical, routine immunoPET for molecular imaging of cell surface biomarkers, based on the most widely used PET radionuclide in current clinical use. The 97% positron yield of  $^{18}\text{F}$  combined with its relatively short half-life offer significant advantages over alternative positron emitters that have been used in conjunction with antibodies. Although radionuclides such as  $^{64}\text{Cu}$ ,  $^{89}\text{Zr}$ , and  $^{124}\text{I}$  have been employed successfully for immunoPET, they exhibit shortcomings. These include significantly lower positron yields, associated gamma and beta emissions, longer physical half-lives that contribute to overall radiation dose, and longer-lived radioactive waste.

The appeal of same-day imaging using  $^{18}\text{F}$ -labeled antibodies, proteins, and peptides has spurred interest in parallel paths that will accelerate progress and broader implementation. McBride et al. developed a novel, facile method for labeling peptides, based on formation of an Al[ $^{18}\text{F}$ ] complex which is then captured by a chelating group such as NOTA (1,4,7-triazacyclononane-1,4,7-triacetic acid) conjugated to a peptide or other targeting moiety [33]. Liu et al. have developed a microfluidic chip for optimization of the coupling of [ $^{18}\text{F}$ ]SFB

to proteins of interest [22]. A digital microfluidic drop generator was designed that enabled computer-controlled metering and mixing of the [ $^{18}\text{F}$ ] tag, biomolecule, and buffer for rapid optimization of labeling conditions. An important next step will be to take full advantage of the Cys-diabody platform, which contains a protected disulfide bridge that can be reduced under mild conditions to release two sulfhydryl groups for site-specific conjugation [16, 18]. Maleimide, vinylsulfone, or other standard thiol-reactive chemistries can be applied to provide stoichiometric, site-specific radiolabeling, instead of coupling to random surface lysine residues, as demonstrated in this work. Alternatively, developments in “click” chemistry for bioconjugation and radiochemistry are also providing innovative new paths to produce novel protein-based molecular imaging tracers [34].

The rapid kinetics observed with the [ $^{18}\text{F}$ ]FB-anti-HER2 diabody during the first 2 h is attractive for same day imaging and confirms the utility of pairing this format with a radionuclide with a 109 min physical half-life. In contrast, intact antibodies have a much longer residence time in blood (~2–3 weeks) and are not optimal agents for imaging, particularly with short half-life radionuclides. Intermediate-sized fragments, such as minibodies, have shown excellent next-day imaging properties [35, 36]. However, the half-life of these fragments (5–11 h) is not compatible with half-life of F-18.

In summary, rapid, routine synthesis of an [ $^{18}\text{F}$ ] tag has been applied for radiolabeling an engineered antibody fragment, enabling rapid immunoPET detection of HER2-expressing tumor xenografts in mice. These labeling approaches will not only be applicable to the highly specialized engineered antibody fragments described here, but can be applied for the rapid and routine radiolabeling of any biomolecule, thus forming the basis of new generations of molecular imaging probes. [ $^{18}\text{F}$ ]FB-diabodies should be highly translatable into a clinical setting, and knowledge gained regarding the molecular and biological characteristics of tumor tissues in patients should aid in the development of personalized cancer treatments.

**Acknowledgments** The authors thank the members of the Wu and Shen labs for their many helpful discussions and contributions. The assistance of Dr. David Stout and Waldemar Ladno of the Crump Institute Small Animal Imaging Facility is greatly appreciated. Funding was provided by National Institutes of Health grants CA086306, CA119367, CA016042; Department of Energy DE-SC0001220, and California Breast Cancer Research Program 14GB-0157. Tove Olafsen and Anna Wu declare a financial interest in ImaginAb, Inc.

**Conflicts of interest** None

## References

1. Wu AM, Olafsen T. Antibodies for molecular imaging of cancer. *Cancer J*. 2008;14(3):191–7.



2. Olafsen T, Wu AM. Antibody vectors for imaging. *Semin Nucl Med.* 2008;40(3):167–81.
3. Nayak TK, Brechbiel MW. Radioimmunoimaging with longer-lived positron-emitting radionuclides: potentials and challenges. *Bioconjug Chem.* 2009;20(5):825–41.
4. Pagani M, Stone-Elander S, Larsson SA. Alternative positron emission tomography with non-conventional positron emitters: effects of their physical properties on image quality and potential clinical applications. *Eur J Nucl Med.* 1997;24(10):1301–27.
5. Smith-Jones PM, Solit DB, Akhurst T, et al. Imaging the pharmacodynamics of HER2 degradation in response to Hsp90 inhibitors. *Nat Biotechnol.* 2004;22(6):701–6.
6. Eder M, Knackmuss S, Le Gall F, et al. 68 Ga-labelled recombinant antibody variants for immuno-PET imaging of solid tumours. *Eur J Nucl Med Mol Imaging.* 2010;37(7):1397–407.
7. Hu S, Shively L, Raubitschek A, et al. Minibody: a novel engineered anti-carcinoembryonic antigen antibody fragment (single-chain Fv-CH3) which exhibits rapid, high-level targeting of xenografts. *Cancer Res.* 1996;56(13):3055–61.
8. Wu AM, Williams LE, Zieran L, et al. Anti-carcinoembryonic antigen (CEA) diabody for rapid tumor targeting and imaging. *Tumor Targeting.* 1999;4:47–58.
9. Williams LE, Liu A, Wu AM, et al. Figures of merit (FOMs) for imaging and therapy using monoclonal antibodies. *Med Phys.* 1995;22(12):2025–7.
10. Cai W, Olafsen T, Zhang X, et al. PET imaging of colorectal cancer in xenograft-bearing mice by use of an <sup>18</sup>F-labeled T84.66 anti-carcinoembryonic antigen diabody. *J Nucl Med.* 2007;48(2):304–10.
11. Vaidyanathan G, Bigner DD, Zalutsky MR. Fluorine-18-labeled monoclonal antibody fragments: a potential approach for combining radioimmunosciintigraphy and positron emission tomography. *J Nucl Med.* 1992;33(8):1535–41.
12. Vaidyanathan G, Zalutsky MR. Labeling proteins with fluorine-18 using *N*-succinimidyl 4-[<sup>18</sup>F]fluorobenzoate. *Int J Rad Appl Instrum B.* 1992;19(3):275–81.
13. Lang L, Eckelman WC. One-step synthesis of 18F labeled [18F]-*N*-succinimidyl 4-(fluoromethyl)benzoate for protein labeling. *Appl Radiat Isot.* 1994;45(12):1155–63.
14. Choi CW, Lang L, Lee JT, et al. Biodistribution of <sup>18</sup>F- and <sup>125</sup>I-labeled anti-Tac disulfide-stabilized Fv fragments in nude mice with interleukin 2 alpha receptor-positive tumor xenografts. *Cancer Res.* 1995;55(22):5323–9.
15. Hou S, Phung DL, Lin W-Y, et al. Microwave-assisted one-pot synthesis of *N*-succinimidyl-4-[<sup>18</sup>F]fluorobenzoate ([<sup>18</sup>F]SFB). *J Vis Exp.* 2011. doi:10.3791/2755.
16. Olafsen T, Cheung CW, Yazaki PJ, et al. Covalent disulfide-linked anti-CEA diabody allows site-specific conjugation and radiolabeling for tumor targeting applications. *Protein Eng Des Sel.* 2004;17(1):21–7.
17. Pietras RJ, Arboleda J, Reese DM, et al. HER-2 tyrosine kinase pathway targets estrogen receptor and promotes hormone-independent growth in human breast cancer cells. *Oncogene.* 1995;10(12):2435–46.
18. Sirk SJ, Olafsen T, Barat B, Bauer KB, Wu AM. Site-specific, thiol-mediated conjugation of fluorescent probes to cysteine-modified diabodies targeting CD20 or HER2. *Bioconjug Chem.* 2008;19(12):2527–34.
19. Defrise M, Kinahan PE, Townsend DW, et al. Exact and approximate rebinning algorithms for 3-D PET data. *IEEE Trans Med Imaging.* 1997;16(2):145–58.
20. Loening AM, Gambhir SS. AMIDE: a free software tool for multi-modality medical image analysis. *Mol Imaging.* 2003;2(3):131–7.
21. Huang SC, Truong D, Wu HM, et al. An internet-based “kinetic imaging system” (KIS) for MicroPET. *Mol Imaging Biol.* 2005;7(5):330–41.
22. Liu K, Lepin EJ, Wang MW, et al. Microfluidic-based <sup>18</sup>F-labeling of biomolecules for immuno-positron emission tomography. *Mol Imaging.* 2011;10(3):168–76.
23. Venisnik KM, Olafsen T, Gambhir SS, Wu AM. Fusion of *Gaussia luciferase* to an engineered anti-carcinoembryonic antigen (CEA) antibody for in vivo optical imaging. *Mol Imaging Biol.* 2007;9(5):267–77.
24. Olafsen T, Sirk SJ, Betting DJ, et al. ImmunoPET imaging of B-cell lymphoma using <sup>124</sup>I-anti-CD20 scFv dimers (diabodies). *Protein Eng Des Sel.* 2010;23(4):243–9.
25. Robinson MK, Doss M, Shaller C, et al. Quantitative immuno-positron emission tomography imaging of HER2-positive tumor xenografts with an iodine-124 labeled anti-HER2 diabody. *Cancer Res.* 2005;65(4):1471–8.
26. Aguilar Z, Akita RW, Finn RS, et al. Biologic effects of heregulin/neu differentiation factor on normal and malignant human breast and ovarian epithelial cells. *Oncogene.* 1999;18(44):6050–62.
27. Rudnick SI, Adams GP. Affinity and avidity in antibody-based tumor targeting. *Cancer Biother Radiopharm.* 2009;24(2):155–61.
28. Lofblom J, Feldwisch J, Tolmachev V, et al. Affibody molecules: engineered proteins for therapeutic, diagnostic and biotechnological applications. *FEBS Lett.* 2010;584(12):2670–80.
29. Baum RP, Prasad V, Muller D, et al. Molecular imaging of HER2-expressing malignant tumors in breast cancer patients using synthetic <sup>111</sup>In- or <sup>68</sup>Ga-labeled affibody molecules. *J Nucl Med.* 2010;51(6):892–7.
30. Kiesewetter DO, Kramer-Marek G, Ma Y, Capala J. Radiolabeling of HER2 specific Affibody(R) molecule with F-18. *J Fluor Chem.* 2008;129(9):799–805.
31. Kramer-Marek G, Kiesewetter DO, Martiniova L, et al. [18F]FBEM-Z(HER2:342)-Affibody molecule—a new molecular tracer for in vivo monitoring of HER2 expression by positron emission tomography. *Eur J Nucl Med Mol Imaging.* 2008;35(5):1008–18.
32. Cheng Z, De Jesus OP, Namavari M, et al. Small-animal PET imaging of human epidermal growth factor receptor type 2 expression with site-specific <sup>18</sup>F-labeled protein scaffold molecules. *J Nucl Med.* 2008;49(5):804–13.
33. McBride WJ, Sharkey RM, Karacay H, et al. A novel method of 18F radiolabeling for PET. *J Nucl Med.* 2009;50(6):991–8.
34. Nwe K, Brechbiel MW. Growing applications of “click chemistry” for bioconjugation in contemporary biomedical research. *Cancer Biother Radiopharm.* 2009;24(3):289–302.
35. Wu AM, Yazaki PJ, Tsai S, et al. High-resolution microPET imaging of carcinoembryonic antigen-positive xenografts by using a copper-64-labeled engineered antibody fragment. *Proc Natl Acad Sci U S A.* 2000;97(15):8495–500.
36. Sundaresan G, Yazaki PJ, Shively JE, et al. <sup>124</sup>I-labeled engineered anti-CEA minibodies and diabodies allow high-contrast, antigen-specific small-animal PET imaging of xenografts in athymic mice. *J Nucl Med.* 2003;44(12):1962–9.